

Macroscopic noise amplification by asymmetric dyads in non-Hermitian optical systems

Alexander Johnston and Natalia G. Berloff*

*Department of Applied Mathematics and Theoretical Physics,
University of Cambridge, Cambridge CB3 0WA, United Kingdom*

(Dated: June 27, 2022)

A strong response to external perturbations or system noise is being exploited for a new generation of sensors, hardware random number generators, and quantum and classical signal detectors. Such applications require the fulfilment of three drastic conditions: macroscopic response to small perturbations, capacity for calibration of imperfections of the system, and fast output data rate. Here, we study the response and noise amplification by asymmetric dyads in freely expanding non-Hermitian optical systems (such as polariton or photon condensates) and show that they fulfil these conditions. We show that by associating the direction of asymmetry with a spin or binary number while coupling several such dyads together leads to systems with required statistical distributions. We show that modifications of the pumping strengths can counteract bias resulting from natural imperfections of the system's hardware and develop the analytical expressions to such corrections to the leading order in asymptotic expansions. Our results suggest that the asymmetric non-Hermitian dyads are promising candidates for efficient sensors and random number generators with controllable statistical properties.

For open quantum and classical systems, it can be justified to consider effective Hamiltonians that are non-Hermitian or non-self-adjoint. The non-Hermiticity of the Hamiltonian implies that the energy eigenvalues are in general complex numbers. In classical optical systems, where resonant frequencies and modes represent energy eigenvalues and eigenstates, non-Hermiticity can enter by gain and dissipation. Non-Hermitian systems driven by gain and dissipation provide a versatile platform for exploring pattern-forming in mechanical and electronic systems, photonics, optics, atomic systems, optomechanics, fluids, biological transport, and acoustics [1–3]. The competition between conservative and non-conservative processes in photonics has led to the creation of disparate artificial structures such as optical fibres [4], photonic crystals [5], metamaterials [6], and exciton-polariton [7] and photon condensates [8]. In such non-Hermitian systems, the discovery of a range of unexpected and unique behaviours was made [9] from topological energy transfer [10, 11] and single-mode lasing [12–14], to robust biological transport [15]. Perhaps one of the most dramatic manifestations of non-Hermitian physics lies in a macroscopic response to small perturbations, e.g., the global asymmetry of spiral waves in Belousov-Zhabotinsky chemical reactions [16], patterns induced by thermal fluctuations just below the onset of convection in fluids [17], or the global direction of vortex rotation or wave chirality in disparate systems governed by the complex Ginzburg-Landau equations [18–20].

Macroscopic amplification of intrinsic microscopic noise provides a way to probe and characterize noise in the system. We distinguish between noise-assisted decay of an unstable state, noisy fluctuations close to an instability onset, and dynamical amplification of unstable states in which fluctuations are dynamically amplified and con-

vected away [21].

Another practical use of noise-sensitive amplification lies in (true) hardware random number generation (hRNG). To be effective for hRNG, the system noise should be statistically random, sampled sufficiently fast, and able to be macroscopically amplified to a measurable level and suitably processed. This is in contrast with pseudo-random number generation implemented by a computer algorithm. Thermal or quantum noise, the photoelectric effect, involving a beam splitter, and other quantum phenomena (e.g., shot noise [22], nuclear decay [23], and spontaneous parametric down-conversion [24]) all can generate low-level, statistically random signals used for hRNG. A series of random numbers are obtained after randomly varying hardware noise is repeatedly sampled with the system-dependent output data rate. True, efficient and fast random number generation is crucial for a variety of industries from cryptography [25–28] to large-scale parallel computation [29] and to the construction of opinion polls and regulation in the electronic gambling industry [30, 31]. Therefore, it is essential to look for novel hardware systems that have non-trivial, statistically controllable and easily detectable macroscopic reaction to the background noise while providing ultra-fast output rate.

In this Letter, we propose that the condensation of freely expanding non-Hermitian condensates, such as microcavity polariton or photon condensates, may have the necessary ingredients (a range of parameters) to be used as sensors, detectors or hRNGs since they fulfil the necessary criteria for efficient operation: macroscopic response to small system noisy perturbations, capacity for calibration of imperfections of the system, and fast output data rate.

Unlike conservative systems, gain-dissipative optical

nonequilibrium systems may have peculiar asymmetric states resulting from fully symmetric conditions even in an ideal system. One of such states is an asymmetric dyad: two geometrically coupled non-Hermitian condensates that possess macroscopic unequal occupations, despite having equal pumping intensities (and other identical conditions) [32]. The degree of population asymmetry varies depending on the losses, nonlinearities, gain intensity and shape, and the distance between the condensates (that all determine the coupling strength) and can be made arbitrarily large or small. The orientation of population asymmetry forms spontaneously in response to any (even insignificant) bias in the system.

We first demonstrate that, starting from random ultra-low-level noisy initial conditions that simulate hardware noise, the two possible directions of the final orientation of the dyad (in terms of its density asymmetry) are equally likely. We develop an error correction scheme and demonstrate that slight modifications of the pumping strength at one condensate site can ensure that both orientations are equally likely even in the presence of small asymmetries in the physical sample itself (that would otherwise bias the results). Following this, we investigate a tetrad structure formed by weakly coupling condensates within two different asymmetric dyads to each other. We show that by modifying these weak, external couplings, one can bias the likelihood of dis-aligned to aligned asymmetric dyads in a precise way. Finally, we present three example chains of dyads in order to demonstrate both uniform and biased statistical distributions.

We model the photonic non-Hermitian system by the following system of N equations describing a network of N optically excited and interacting nonequilibrium condensate centres (CCs):

$$\dot{\psi}_i = -i|\psi_i|^2\psi_i - \psi_i + (1 - ig) \left[\left(\frac{\gamma}{1 + \xi|\psi_i|^2} \right) \psi_i + \sum_{j \neq i} J_{ij} \psi_j \right], \quad (1)$$

where $\psi_i(t) = \sqrt{\rho_i} \exp[i\theta_i]$ is the complex amplitude of the i^{th} CC (and ρ_i and θ_i are its occupation and phase, respectively), γ is the pumping strength, g is the detuning strength (blueshift), ξ characterises the relative strength of the system's nonlinearities, and J_{ij} is the coupling strength between the i^{th} and j^{th} CCs. Typically $|J_{ij}| < 1$ in these dimensionless units. These equations describe a variety of coupled oscillator systems with saturable nonlinearity, from nonequilibrium condensates (such as polariton or photon condensates) to lasers and non-parametric oscillators [18, 32–34]. These equations can be derived using the tight-binding approximation of the mean-field complex Ginzburg-Landau equation in the fast reservoir regime [32, 34] or using the full mean-field Maxwell-Bloch equations for laser cavities [35]. The system exhibits a range of behaviours depending on system parameters such as evolution to a stationary state, periodic or chaotic oscillations [32, 33]. The combination

of nonlinearity, gain, and dissipation in such systems results in a region of parameter space in which the density and phase asymmetry of stationary states appears even with identical site conditions, as a result of quantum or classical noise amplification. Fig. 1(a) shows the region in $g - |J| - \xi$ space in which asymmetric states occur for the system described by Eq. 1, for three values of γ . The three surfaces bound the region from above (in terms of ξ) in each case. For a dyad in such a parameter regime, the two possible configurations for the resultant population asymmetry are equally likely under ideal conditions and can be identified in binary representation, e.g., with either a “1” or a “0” depending on the direction of asymmetry.

Error correction. In reality, the physical sample on which the condensates are prepared will likely have some intrinsic asymmetry, which may result in a slight preference for the higher-density component of the asymmetric dyad to condense at one site in particular. Below we show that it is possible to counteract such intrinsic asymmetry by modifying the pumping strength applied to one of the condensates.

We model asymmetry in the physical sample by considering a small perturbation ϵ to g for one of the condensates given by Eq. 1. We show that it is possible to modify the pumping strength of this condensate $\tilde{\gamma}$ to again achieve an equally-likely distribution of asymmetry in the dyad. The steady state of such a dyad satisfies:

$$-i\mu\psi_1 = -i|\psi_1|^2\psi_1 - \psi_1 + (1 - ig) \times \left[\left(\frac{\gamma}{1 + \xi|\psi_1|^2} \right) \psi_1 + J\psi_2 \right], \quad (2)$$

$$-i\mu\psi_2 = -i|\psi_2|^2\psi_2 - \psi_2 + (1 - i(g + \epsilon)) \times \left[\left(\frac{\tilde{\gamma}}{1 + \xi|\psi_2|^2} \right) \psi_2 + J\psi_1 \right], \quad (3)$$

where μ is the chemical potential defined by $i\dot{\psi}_i = \mu\psi_i$ and ψ_i are the new condensate wavefunctions modified from their steady-state values of Eq. 1. We will consider small deviations from the unperturbed values marked by superscript 0 by writing $\psi_1 = a_1^0 + \epsilon a_1^1$, $\psi_2 = (a_2^0 + \epsilon a_2^1) \exp(i\theta^0 + i\epsilon\theta^1)$ with the chemical potential $\mu = \mu^0 + \epsilon\mu^1$ and pumping $\tilde{\gamma} = \gamma^0 + \epsilon\gamma^1$. We then linearize Eqs. (2) and (3) for small ϵ . To the leading order we recover the steady states of Eq. (1)

$$-i\mu^0 = -i(a_j^0)^2 - 1 + (1 - ig) \left[\frac{\gamma^0}{1 + \xi(a_j^0)^2} + J \frac{a_l^0}{a_j^0} \exp(i(-1)^j \theta^0) \right], \quad (4)$$

where $j = 1, l = 2$ or $j = 2, l = 1$. At the first order in small ϵ , we get four real linear equations that we can solve for a_1^1, a_2^1, γ^1 and θ^1 , while keeping μ^1 as a free parameter. The expression for γ^1 should be invariant under the change $a_1^0 \longleftrightarrow a_2^0, \theta^0 \longleftrightarrow -\theta^0$. This consider-

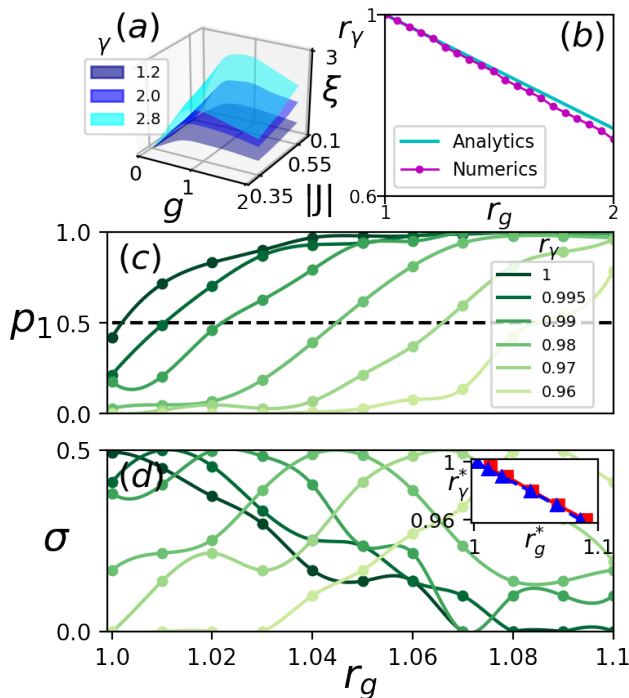


FIG. 1. (a): Surfaces defining upper bounds (in terms of ξ) of the regions of $g - |J| - \xi$ space in which asymmetric dyads form, for three values of γ . The regions are symmetric with respect to the sign of J . For each value of γ , the set of N equations described by Eq. 1 was solved for $N = 2$ (with random initial conditions) for 12500 sets of parameters within the $g - |J| - \xi$ space shown. A smooth surface was then fitted at the boundary of the set of points at which asymmetric states were stable. For a dyad with equal occupations, (b) shows the relationship between the ratios $r_g \equiv (g + \epsilon)/g$ and $r_\gamma \equiv \tilde{\gamma}/\gamma^0$ required to maintain equal occupation. r_g (r_γ) represents the ratio of the blueshift (pumping strength) between the two condensate sites. The analytical approximation of Eq. 5 for small ϵ (i.e. $r_g \approx r_\gamma \approx 1$) is compared against numerically-calculated values. The parameters used in (b) are $J = 0.45$, $\gamma = 1.8$, $g = 0.4$, and $\xi = 2$. (c) and (d): The proportion of times the system converges to a “1” state, p_1 , as a function of r_g for a variety of values of r_γ is shown in (c). Here $p_1 \equiv n_1/(n_0 + n_1)$, where n_1 (n_0) is the total number of “1” (“0”) states the system converges to. The standard deviation of the set of final states, σ , as a function of r_g is shown in (d) for the same values of r_γ . Each data point was calculated by running 1000 simulations of the set of N equations described by Eq. 1 for $N = 2$ with random initial conditions and a single coupling, J , between the two condensates. For each value of r_γ , there is a critical point $r_g = r_g^*$ at which $p_1 = \sigma = 0.5$ - the scenario describing a fair coin toss. The inset of (d) shows a plot of these critical points (r_γ^*, r_g^*) determined empirically using cubic spline methods from (c) when $p_1 = 0.5$ (blue triangles) and (d) when $\sigma = 0.5$ (red squares). For (c) and (d), $J = 0.55$, $\gamma = 2.8$, $g = 0.5$, and $\xi = 5/3$.

ation fixes the value of μ^1 and shows that it is possible to modify the pumping by γ^1 to compensate for the asymmetry in the cavity blueshift, g . Simpler analytics can

be obtained by considering the limit of small asymmetry between the condensates: $a_2^0 = (1 + \delta)a_1^0$, $\delta \ll 1$. To the leading order in δ , Eq. (4) gives the unperturbed solutions $(a_1^0)^2 = (\gamma^0 + |J| - 1)/(1 - |J|)\xi$, $\theta^0 = 0$ (for $J > 0$) and $\theta^0 = \pi$ (for $J < 0$) and $\mu^0 = g + (a_1^0)^2$. These states correspond to the states of equal occupancy. Considering the leading order expansions in δ of the first order equations in small ϵ , we get

$$\gamma^1 = -\frac{g\gamma^0}{(1+g^2)(1-|J|)}, \mu^1 = \frac{1}{2} - \frac{\gamma^0 g}{2(1+g^2)(1-|J|)^2 \xi},$$

$$\theta^1 = \frac{1}{2(1+g^2)|J|}. \quad (5)$$

Fig. 1(b) shows the values of the ratios $r_g \equiv (g + \epsilon)/g$ and $r_\gamma \equiv \tilde{\gamma}/\gamma^0$ required to maintain equal occupation. Values derived using the analytical approximation of Eq. 5 are shown alongside numerically-calculated values.

When δ is not small, we numerically investigate the effect of r_g and r_γ on the proportion of “1” states produced, $p_1 \equiv n_1/(n_0 + n_1)$, where n_1 (n_0) is the total number of “1” (“0”) states the system converges to after 1000 trials. Fig. 1(c) shows a series of curves depicting this proportion as a function of r_g for a range of values of r_γ , while Fig. 1(d) shows the standard deviation of the set of spin values (i.e. 0, 1) collected. When $r_g = r_\gamma = 1$, $p_1 = \sigma = 0.5$, as expected from a binomial distribution with $p = 0.5$, i.e. a fair coin toss. Increasing r_g , causes p_1 to increase towards a plateau at which all states are “1” states. Decreasing r_γ , however, counteracts this effect, shifting the starting point of the curve such that $p_1 < 0.5$ when $r_g = 1$. Since p_1 increases as r_g increases, this ensures that there is always an optimum pair of values (r_g^*, r_γ^*) at which $p_1 = \sigma = 0.5$. Cubic spline methods were used to empirically determine a set of six (r_g^*, r_γ^*) values in the case when $p_1 = 0.5$ and when $\sigma = 0.5$, respectively. An inset in Fig. 1(d) shows a plot of r_γ^* against r_g^* calculated using $p_1 = 0.5$ intersection points (blue triangles) and $\sigma = 0.5$ intersection points (red squares). For this range of perturbed values of g , the analytics obtained to the first order in ϵ gives the correct numerically observed slope of -0.448 . It is therefore possible to counteract the effect of any intrinsic asymmetry in the physical sample by appropriately modifying the pumping strength at one site. In this way the system can be engineered to ensure that the resultant orientation of population asymmetry within an asymmetric dyad statistically resembles the behaviour of a perfectly fair coin toss. In addition, a chain of such dyads, constructed such that the coupling is zero between condensates in different dyads, would ensure the orientation of each individual dyad is independent of all the others. These two facts (the system’s unbiased choice of dyad asymmetry orientation and the independence of individual dyads) enable a chain of such dyads to be used to produce uniform random number distributions (as we demonstrate later). It

also means that such a system could potentially be used as a sensitivity device. Once the unbiased platform is set up, any subsequent asymmetry in the orientation statistics could be attributed to the presence of some internal defect in the sample or (if one condensate is shielded) an external effect (e.g. low-intensity radiation) which temporarily biases the results. This would allow one to map when such external effects impact the dyad.

We now consider a tetrad configuration in which two asymmetric dyads are weakly coupled to each other [32]. In this arrangement, there is a coupling J between condensates in each asymmetric dyad, while adjacent condensates (i.e. those within different asymmetric “dyads”) are coupled with strength αJ where $\alpha \ll 1$. This arrangement is outlined in Fig. 2(a). In previous work [32], the highest occupation (ground) states of this configuration were investigated. However, all possible states (11, 10, 01, and 00) are possible depending on the initial conditions and α . Fig. 2(a) shows these four states, while Fig. 2(b) shows the proportion, p , of times each state forms over 10000 trials with random initial conditions, for a range of values of α . When $\alpha = 0$ (i.e., when we have two non-interacting dyads) all possible arrangements are equally likely, as expected. However, when α is nonzero, there is a bias towards dis-aligned states (i.e. those representing 10 and 01). The inset of Fig. 2(b) shows that this bias - defined as $B \equiv p_{\text{dis-aligned}}/p_{\text{aligned}}$ where $p_{\text{dis-aligned}}$ (p_{aligned}) is the proportion of dis-aligned (aligned) states - increases with α in a nonlinear fashion. Crucially, one can bias the distribution to a significant extent ($B \approx 4$ when $\alpha = 0.1$). If the reciprocal bias is desired, the sample can simply be arranged such that the couplings between dyads cross so that the tetrad forms an “X” shape rather than a square. This arrangement is shown in the following section (specifically, Fig. 4(c)). Ultimately, such tetrads form the fundamental unit in larger chains of dyads that enable customised probability distributions to be generated by modifying couplings between dyads along the chain.

A chain of N asymmetric dyads has 2^N possible arrangements, which (since each dyad can be considered as a bit) correspond to the integers $0, 1, 2, \dots, 2^N - 1$. Fig. 3 depicts the densities and relative phases of the chain of 30 condensate dyads with no couplings between neighboring dyads. The chain represents the integer 679,416,442 in its decimal representation.

By modifying the coupling strength between dyads it is possible to bias the resultant distribution of numbers generated by the chain. Such couplings can be either lateral (in which the upper condensate of one dyad is coupled to the upper condensate of the adjacent dyad, and the same for the lower condensates) or crossed (in which the upper condensate within one dyad is coupled to the lower condensate of the adjacent dyad and vice versa). Note that such control can be achieved by exploiting the fact that

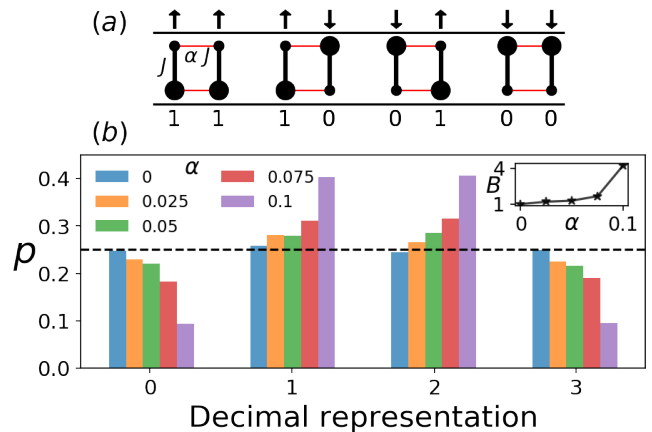


FIG. 2. The arrangement of the tetrad system for the four possible final states obtained by numerical integration of Eqs. (1) are shown in (a). Larger (smaller) circles denote higher (lower) density condensates. Thick black (thin red) lines show the coupling J between condensates within an asymmetric dyad (between condensates in different asymmetric dyads). (b) shows a histogram of the proportion, p , of times the system converges to each of the four states, categorised by their decimal representation, for five values of α . The unbiased case, $p = 0.25$, is shown with a dashed black line. For each value of α , the set of N equations described by Eq. 1 was solved for 10000 random initial conditions, with $N = 4$ and the J_{ij} coupling matrix elements as prescribed by the diagrams in (a). The inset shows the bias, B (the ratio between the proportion of dis-aligned states to that of aligned states) as a function of α . Here $J = 0.55$, $\gamma = 2.8$, $g = 0.5$, and $\xi = 5/3$.

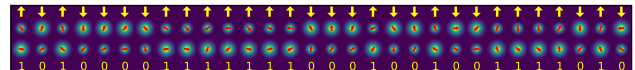


FIG. 3. Arrangement of an $N = 30$ chain of asymmetric dyads with no couplings between neighboring dyads. Condensate densities are depicted in a blue (low)-yellow (high) colour scheme while their respective phases are shown with red arrows. The spin representation (from the dyads’ density asymmetry) is shown above the condensates with yellow arrows while the binary representation of each dyad is shown below. Overall, the chain represents the integer 679,416,442 in its decimal representation.

the coupling strength between two dyads as a function of their separation distance behaves as a Bessel function [36]. Thus, adjustments to the spacing between pumping sites can achieve either lateral or crossed couplings between dyads in the chain. Finally, it is also possible to completely eliminate certain sections of the random number distribution by increasing the pumping strength of one condensate of one or more dyads, thus making its orientation deterministic. Fig. 4 illustrates three example distributions. Fig. 4(a) is a uniform distribution created with a chain of non-interacting dyads. Figs. 4(b) and (c)

show biased distributions, making use of couplings between dyads and modified pumping strengths in order to bias the resultant random number distribution.

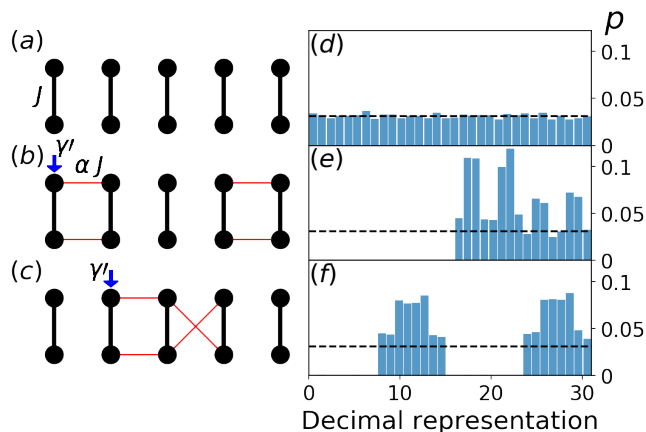


FIG. 4. Three chains of asymmetric dyads [(a),(b),(c)] numerically computed using Eq. (1) for $N = 10$ shown alongside their associated probability distributions [(d),(e),(f)]. Distributions are calculated by categorising decimal representations of the final configurations of the system using 5000 random initial conditions. The unbiased case, $p = 1/32$, is shown with a dashed black line in each plot. The coupling strengths J_{ij} are prescribed by the corresponding diagrams [(a),(b),(c)]. Circles mark where condensates form, while blue arrows show sites at which an increased pumping strength, $\gamma' = 1.05\gamma$, is used. Thick black lines show couplings of strength J while thin red lines show weaker couplings of strength αJ . (a) shows a chain of non-interacting dyads, producing a uniform random number distribution (d). The biased distributions of (e) and (f) result from the design of the chains in (b) and (c). (b) shows a chain with two lateral couplings with strength $\alpha = 0.1$ and increased pumping strength at one site. (c) shows a chain with one set of lateral couplings and one set of crossed couplings, both of which have $\alpha = 0.01$, and one site with increased pumping strength. In all simulations $J = 0.55$, $\gamma = 2.8$, $g = 0.5$, and $\xi = 5/3$.

In summary, we have elucidated a simplest case of macroscopic response that leads to density asymmetry in a photonic non-Hermitian dyad and suggest that these structures can be used in sensitivity devices and for hRNG, among many other noise-dependent applications. Error correction for unbiased statistics of the dyad orientations are possible with this system, since any bias resulting from asymmetry in the sample can be overcome by modifying the pumping strength at one condensation site. Such systems could be used to sense irregularities both internal and external to the sample. Unbiased orientations enable the generation of uniform random number distributions while controlled bias can be introduced by implementing weak couplings between condensates in different dyads. Finally, with potentially hundred of thousands of the asymmetric dyads placed on a chip, and due to the ultra-short picosecond coherence times of laser and

polariton condensates, the sampling of low-level, statistically random signals will occur in parallel and at an ultra-fast timescale, bringing the random number generation comfortably to the THz regime, bounded only by the speed of conversion of the signal to the electronic domain.

Acknowledgements. A.J. is grateful to Cambridge Australia Scholarships and the Cambridge Trust for entirely funding his Ph.D. N.G.B. acknowledges the financial support from the John Schwinger Foundation Grant No. JSF-19-02-0005.

-
- * correspondence address: N.G.Berloff@damtp.cam.ac.uk
- [1] H.-J. Stöckmann, E. Persson, Y.-H. Kim, M. Barth, U. Kuhl, and I. Rotter, *Physical Review E* **65**, 066211 (2002).
 - [2] C. E. Rüter, K. G. Makris, R. El-Ganainy, D. N. Christodoulides, M. Segev, and D. Kip, *Nature physics* **6**, 192 (2010).
 - [3] J. Wiersig, *Physical Review A* **84**, 063828 (2011).
 - [4] J. C. Knight, J. Broeng, T. A. Birks, and P. S. J. Russell, *Science* **282**, 1476 (1998).
 - [5] J. D. Joannopoulos, P. R. Villeneuve, and S. Fan, *Nature* **386**, 143 (1997).
 - [6] V. M. Shalaev, *Nature Photonics* **1**, 41 (2007).
 - [7] J. Kasprzak, M. Richard, S. Kundermann, A. Baas, P. Jeambrun, J. Keeling, F. Marchetti, M. Szymańska, R. André, J. Staehli, *et al.*, *Nature* **443**, 409 (2006).
 - [8] J. Klaers, J. Schmitt, F. Vewinger, and M. Weitz, *Nature* **468**, 545 (2010).
 - [9] R. El-Ganainy, K. G. Makris, M. Khajavikhan, Z. H. Musslimani, S. Rotter, and D. N. Christodoulides, *Nature Physics* **14**, 11 (2018).
 - [10] H. Xu, D. Mason, L. Jiang, and J. Harris, *Nature* **537**, 80 (2016).
 - [11] S. Ghosh and Y. Chong, *Scientific Reports* **6**, 1 (2016).
 - [12] H. Hodaei, M.-A. Miri, M. Heinrich, D. N. Christodoulides, and M. Khajavikhan, *Science* **346**, 975 (2014).
 - [13] M.-A. Miri, P. LiKamWa, and D. N. Christodoulides, *Optics Letters* **37**, 764 (2012).
 - [14] L. Feng, Z. J. Wong, R.-M. Ma, Y. Wang, and X. Zhang, *Science* **346**, 972 (2014).
 - [15] D. R. Nelson and N. M. Shnerb, *Physical Review E* **58**, 1383 (1998).
 - [16] S. C. Müller and T. Plesser, in *Chemical Waves and Patterns* (Springer, 1995) pp. 57–92.
 - [17] I. Rehberg, S. Rasenat, M. De La Torre Juarez, W. Schöpf, F. Hörner, G. Ahlers, and H. Brand, *Physical review letters* **67**, 596 (1991).
 - [18] K. Staliunas and V. J. Sanchez-Morcillo, *Transverse patterns in nonlinear optical resonators*, Vol. 183 (Springer Science & Business Media, 2003).
 - [19] J. Keeling and N. G. Berloff, *Physical Review Letters* **100**, 250401 (2008).
 - [20] S. N. Alperin and N. G. Berloff, *Optica* **8**, 301 (2021).
 - [21] M. Santagiustina, P. Colet, M. San Miguel, and D. Walgraef, *Physical review letters* **79**, 3633 (1997).
 - [22] Y. Shen, L. Tian, and H. Zou, *Physical Review A* **81**,

- 063814 (2010).
- [23] M. Herrero-Collantes and J. C. Garcia-Escartin, *Reviews of Modern Physics* **89**, 015004 (2017).
- [24] A. Marandi, N. C. Leindecker, K. L. Vodopyanov, and R. L. Byer, *Optics Express* **20**, 19322 (2012).
- [25] C. S. Petrie and J. A. Connelly, *IEEE Transactions on Circuits and Systems I: Fundamental Theory and Applications* **47**, 615 (2000).
- [26] K. Yoshimura, J. Muramatsu, P. Davis, T. Harayama, H. Okumura, S. Morikatsu, H. Aida, and A. Uchida, *Physical Review Letters* **108**, 070602 (2012).
- [27] H. Koizumi, S. Morikatsu, H. Aida, T. Nozawa, I. Kakesu, A. Uchida, K. Yoshimura, J. Muramatsu, and P. Davis, *Optics Express* **21**, 17869 (2013).
- [28] T. Honjo, A. Uchida, K. Amano, K. Hirano, H. Someya, H. Okumura, K. Yoshimura, P. Davis, and Y. Tokura, *Optics Express* **17**, 9053 (2009).
- [29] H. Miyazawa and M. Fushimi, in *Proceedings of the International Symposium on Operations Research and Its Applications* (Citeseer, 2009) pp. 448–452.
- [30] C. Rousseau and Y. Saint-Aubin, in *Mathematics and Technology* (Springer, 2008) pp. 1–23.
- [31] H. G. Katzgraber, arXiv preprint arXiv:1005.4117 (2010).
- [32] A. Johnston, K. P. Kalinin, and N. G. Berloff, *Physical Review B* **103**, L060507 (2021).
- [33] I. Aleiner, B. Altshuler, and Y. G. Rubo, *Physical Review B* **85**, 121301 (2012).
- [34] K. P. Kalinin and N. G. Berloff, *Physical Review B* **100**, 245306 (2019).
- [35] A. Dunlop, W. Firth, D. Heatley, and E. M. Wright, *Optics Letters* **21**, 770 (1996).
- [36] H. Ohadi, R. Gregory, T. Freearde, Y. Rubo, A. Kavokin, N. Berloff, and P. Lagoudakis, *Physical Review X* **6**, 031032 (2016).